Sharpening of Natural Stars Using Deployable Laser Guide Stars for NGAO

KECK ADAPTIVE OPTICS NOTE 635

Christopher Neyman[a] and Richard Dekany[b]

[a]W. M. Keck Observatory, 65-1120 Mamalahoa Hwy., Kamuela, HI 96743
[b]California Institute of Technology, Pasadena, CA 91125

ABSTRACT

A conventional single laser guide star (LGS) adaptive optics (AO) system generally requires additional tip/tilt information derived using natural guide stars (NGS). Multi-LGS systems will benefit from measurement of additional low-order modes using one or more natural stars. If the NGS's are partially corrected by the LGS AO system, the compensated image results in both improved AO tracking performance and greater accessible sky fraction. Multi-object adaptive optics (MOAO) sharpening of NGS is possible where a good estimate of the NGS wavefront can be made in those cases when laser guide star tomographic information is available. We describe an approach based on additional patrolling laser beacons that are dedicated to sharpening available natural guide stars. Simulations for several noise free cases are presented. In addition, information relating to finite signal to noise ratio data is also presented.

1. Introduction

The concept of using deployable LGS to improve the sky coverage of NGAO was first proposed by Dekany [1] in KAON 504. The concept was named "Point and Shoot" LGS in that report. That report showed a favorable impact on sky coverage with the "Point and Shoot" (P&S) concept. However, KAON 504 was limited in scope, it used only the NGAO error budget spreadsheet. As such, the analysis considered the deployable LGS as a limiting case of a regular LGS asterism expanded to optimize sky coverage at the expense of on-axis science performance. The study used the tomography errors from earlier NGAO trade studies [2, 3] extrapolated to larger radii. In addition, the original study assumed that the LGS measurement error would decrease as the square root of the number laser spots used in the asterism. The NGAO team decided to improve our understanding of the P&S concept by undertaking a more complete set of Monte Carlo simulations.

The goals for this follow on study were to understand the following effects:

- Performance gain when the P&S LGS is used in the on axis tomography solution
- Performance loss when the P&S LGS is not used in the tomography solution
- LGS asterism that best balance sky coverage and on-axis performance
- Optimal placement of the P&S LGS relative to the natural stars
- Effects of finite signal to noise and correction update rate on performance

We have been successful on the main points of this study with the exception of a complete understanding of the effects of finite signal to noise on the tomographic correction. Some preliminary results of this study were presented at the SPIE 2008 in Marseille [4] and published as KAON 601 [5]. We will review and give a more complete reporting of these results in sections two and three. The issues related to noise scaling originally proved puzzling. We naively assumed that the LGS measurement error for a tomographic reconstructor would decrease as the square root of the number laser spots used. Simulations that explore this phenomenon are discussed in section 4. A theoretical explanation of this effect was developed by Gavel [6] and is the subject of KAON 621. We have not completed an exhaustive simulation of noise propagation effects in LGS simulations. That will be the subject of future investigations. This work was part of the preliminary design phase of NGAO, a standard phase of new instrument development at W. M. Keck Observatory. The results in this KAON are part of NGAO WBS 1.3.3.3.2.1 the Tip Tilt Sharpening Study.

1.1. MCAO and MOAO sharpening

Multiconjugate AO (MCAO) has been proposed as a method of sharpening field NGS to improve the quality of low-order measurements. To obtain the highest sky coverage, we must select field NGS from a field diameter extending over two arc minutes or more[1]. Generalized anisoplanatism limits the ability of simple dual-conjugate MCAO systems to provide good sharpening over such a large field of regard. Extension of MCAO to three-conjugate correction or more could theoretically improve field NGS sharpening, but this increases the complexity of MCAO system optical design. Maintaining small pupil aberrations while relaying a wide field of view is difficult, particularly for large aperture telescopes. The inclusion of additional DM's in series also introduces additional transmission losses and complications in the MCAO control law.

Multiobject AO (MOAO) provides an attractive alternative to MCAO for the purpose of field NGS sharpening. In the MOAO paradigm, a separate deformable mirror is dedicated to each object of interest, allowing wavefront correction calculated specifically for that direction in the sky. Because each target can be corrected individually, MOAO eliminates generalized anisoplanatism error. In exchange, MOAO increases computational hardware requirements, as the tomographic wavefront estimate must be calculated in each target direction. Furthermore, because each DM correction is applied without optical feedback to the high-order wavefront sensor paths, MOAO correction must be applied using a 'go-to' control, requiring excellent calibration and stability of all DM's and high-order WFS.

An alternative approach, being pursued by the NGAO team is to combine MOAO sharpening with pupil-conjugated deformable mirror correction based on laser tomography AO (LTAO). In this hybrid approach, the first LTAO stage applies a relatively low-order correction to the entire field of view, using a moderate format DM in a common pupil. Subsequent to this, MOAO correction is applied in the direction of each field NGS, using a dedicated MEMs deformable mirror. The hybrid LTAO/MOAO approach to sharpening field NGS has several advantages. Whereas a classical MOAO system would need to correct both static telescope and atmospheric wavefront errors, the hybrid approach requires MOAO correction of only the anisoplanatic component of the wavefront error. In many cases, this reduces the dynamic range and linearity requirements on the MOAO correctors. Because the high-order WFS light can be made to enjoy this same first stage LTAO correction, feedback on the shared DM shape is provided, forming a quasi-closed-loop system.

2. Tomography error from Fixed vs. Patrolling LGS

When MOAO sharpening natural guide stars the fundamental limit is tomography error: the ability to estimate and correct turbulence in the direction of the NGS. Errors will arise due to uncertainties in the turbulence height, missing wavefront information, and errors arising from blind modes.

In the NGAO hybrid LTAO/MOAO approach, we seek to optimize the total science target wavefront correction, as a combination of the tomography error on-axis and the residual low-order wavefront sensing error using sharpened field stars. The on-axis tomography error directly influences the science sensitivity, while the off-axis field NGS tomography error reduces sharpening and increases low-order mode measurement error decreasing sky coverage and indirectly degrading science target sensitivity.

To date fixed LGS asterisms have been favored for large telescope LTAO and MCAO systems. This is because good wavefront correction is needed in both the science target direction and in the directions of each of the field NGS used for low-order wavefront sensing. The radii of these LGS asterisms have typically been selected to provide a reasonable compromise between the tomography error on-axis and that across the background star field.

NGAO proposes the use of a reconfigurable LGS asterism to provide near-optimal tomographic wavefront sensing for the on-axis science target direction and for each field NGS direction simultaneously. We expect improved tomographic correction near each LGS, where the tomographic interpolation/extrapolation from the instantaneously measured wavefront directions is minimized. In this approach, LGS light can be portioned into a smaller fixed LGS asterism, optimized for tomography in the on-axis science direction, and a patrolling LGS asterism configured to provide the best field NGS sharpening on a target-by-target basis.

3. Methodology

Simulations in this paper were performed with the LAOS simulation developed by the Thirty Meter Telescope project. LAOS is a complete Monte Carlo AO simulation that performs both an explicit tomography step to estimate the volume of turbulence above the telescope and a fitting step that determines the correction to apply based on a user selectable set of evaluation points. In the case of MOAO, i.e. several LGSs and one DM per target, the fitting step is optimized for each target point (science or NGS) independently. In the case of MCAO, i.e. several LGS and a few DMs correcting all field points simultaneously, the correction is based on user selectable weighting to optimize the correction over the field of view using a finite number of deformable mirrors. LAOS simulations were performed that isolate the effect of tomography from other AO system errors.

The spacing of the actuator grid and the size of the subapertures was set to 0.3516 m. This spacing results in approximately 32 subapertures and 33 actuators across the Keck pupil. In order to isolate the tomography error, the simulations were noise free and the system had an infinite correction bandwidth that is a zero time delay between measurement and correction of the wavefront. The atmospheric Cn^2 profile and wind speed were the Mauna Kea summit ridge model with r_0 = 16 cm and θ_0 = 2.70 arc seconds.

Single star NGS simulations with the same phase screen seeds were run to estimate the effect of the fitting error with 32 actuators across the pupil. The tomography error was estimated by taking each LGS run and subtracting the NGS results in quadrature. The results from the five random seeds were averaged to get the result; each seed was run until the AO loop achieved stable performance. Tomography performance was evaluated at 49 points on a rectangular grid with 20 arc second spacing between points; the boundary of the sample points was a square 120 arc seconds on a side. Other sample points were selected at the location of the laser guide stars and at other key locations located in the outskirts of LGS constellation.

4. Regular constellation comparison

In order to estimate the effect of using 3 deployable LGS that would be pointed close to a NGS located in the outer edges of the NGAO field of view and 3 lasers in a compact triangle to correct an on axis science object, we compared this asterism to others we had simulated in the past. These asterisms are referred to using the naming scheme of Ralf Flicker from KAON 429 [2]. The 3 LGS in a ring is known as 3a. Another asterism that showed vey small tomography error in this study was 9c, which is two interlinking boxes of LGS in addition to a single LGS placed at the center. We also used the “Pentagon plus One” asterism favored in early NGAO design studies. We approximate a true point and shoot asterism as a combination of two 3a asterisms. The inner one corrects the on axis science wavefront and the outer ring is used to correct the NGS wavefront. The performance of the 3a 20” + 3a 60” was found to be weakly dependent on rotation of the two asterism relative to each other. The tomography error from these asterisms is shown in Figures 1-4. Unfortunately, the contour plots are not shown on the same color map for easier comparison. The tomography error at each of the evaluation points (plus signs in the contour plots) is plotted as function of radial distance in Figure 5 for three of the candidate asterisms. One can conclude from the figure that the 3a asterism with deployable outer LGS performs almost as well on axis as the 9c asterism and its performance in the direction of the LGS is comparable to the 9c asterism. As expected in directions away from the LGS, the 3a asterism performs poorly. The next plot, Figure 6, shows a comparison of a 50 and 20 arc second radius Pentagon asterisms and the 3a asterism. The larger pentagon asterism gives better results overall but the 3a asterism is superior in the direction of the NGS. A comparison of pentagon asterisms of varying radius is shown in Figure 7. A clean comparison between the 3a asterism and the 50 arc second radius pentagon is shown in Figure 8. Pentagons of 30 and 50 arc seconds radius are compared in Figure 9.

5. Optimized patrolling LGS placement

We are further interested in knowing, for any given field NGS off-axis distance, what is the optimum direction to which to point a patrolling LGS to affect the greatest MOAO sharpening, through reduction of tomography error.

The situation was investigated briefly by performing two LAOS simulations with 3a 20 + 3a XX configurations where the outer radius was set at values of 60 and 70 arc seconds respectively. The tomography error contours are shown in Figure 10 and Figure 11. A plot of the tomography error is also shown in Figure 12. As seen in figures the tomography error for a typical field NGS, at a field location of 60 arc seconds is indeed minimized (both locally and absolutely) by pointing the patrolling LGS several arc seconds outside the nominal field NGS location. A more complete discuss of this effect is given in the SPIE paper [4] and KAON 601 [5].

6. Noise scaling studies

Noise propagator is the ratio of the standard deviation of the noise in the estimate of wavefront along the direction of a guide star to the standard deviation in the noise of the measurement. One way to determine the noise propagator is from the root sum square-difference of an estimate to the zero noise case. Another way, for linear systems, is to simply have zero atmospheric index fluctuation (r_0=infinity) and assess the response to measurement noise. In the simulations reported on below, we have used the first method.

Noll, Fried, and others have shown that single guide star noise is dependent on the number of subaperture n_{sa}, and on centroid error, σ_θ as:

$$\sigma^2_{noise} \propto \ln(n_{sa})\sigma^2_\theta \qquad (1)$$

Our original attempt to add the effects of finite signal to noise ratio into the point and shoot simulations proved puzzling. They did not follow our naïve expectation that the effective centroid error in multi LGS analog of eq. (1) would be equal to the centroid error of a single laser divided by the number of lasers. In fact, our full tomography simulations show about the same performance (a floor) with more guide stars. Our results were only weakly dependant on guide star numbers. Simulations included (4-7 LGS) on a single ring with one LGS at the center are shown in Figure 13. The error plotted in that figure represents the quadrature difference between a noisy and a noise free simulation that are otherwise identical.

Following up on a suggestion by Don Gavel, we performed a simulation with 3 LGS on a ring of expanding radius. In particular, when the ring radius is zero and the LGS are at the same location, the simulation should be equivalent to single guide star that is 3 times brighter. As the radius increases, the noise will approach the case of single guide star. This is because the wavefront of each LGS no longer overlap and the measurements become statistically independent.

A similar behavior was observed in UCSC at the Laboratory for Adaptive optics. Don Gavel has developed a theoretical explanation for this effect; see more details in KAON 621. The conclusions of that report are that adding more guide stars can serve one of two purposes.

1) Introducing denser sampling of the atmosphere, in which case the noise propagator remains unity. That is increasing noise with decreasing power per guide star.
2) Alternatively, it introduces measurement redundancy, in which case the noise propagator follows the law of averages and decreases with increasing laser power per guide star.

The study concludes, however, that it cannot do both simultaneously.

7. Practical considerations

A number of practical considerations are also important in the use of point and shoot LGS. We list the following issues:

- Optomechanical complexity increased
- Reconstructor generation
- Observational efficiency
- Sequencer and system complexity

These items are discussed in more detail in the SPIE paper [4] and KAON 601 [5].

8. Conclusions

This study gives results for the expected tomography error when deployable beacons are used. The goals for this follow on study were to understand the following effects:

- Performance gain when the P&S LGS is used in the on axis tomography solution
- Performance loss when the P&S LGS is not used in the tomography solution
- LGS asterism that best balances sky coverage and on-axis performance
- Optimal placement of the P&S LGS relative to the natural stars

We have only reached a basic understanding of the effect of noise. In addition, all studies to date have assumed uniformly spaced lasers in the outer ring. In reality, any viable patrolling LGS strategy would need to be verified considering actual asymmetric patrolling asterisms.

References

1. R. Dekany, NGAO Performance vs. Technical Field of View for LOWFS Guide Stars, Keck Adaptive Optics Note 504, (W. M. Keck Observatory, Kamuela, Hawaii, 2007).
2. R. Flicker, “NGAO Trade Study Report: LGS Asterism Geometry and Size,” Keck Adaptive Optics Note 429, (W. M. Keck Observatory, Kamuela, Hawaii, 2006).
3. D. Gavel and C. Neyman, “Tomography Codes Comparison and Validation”, Keck Adaptive Optics Note 475, version 2, (W. M. Keck Observatory, Kamuela, Hawaii, 2007).
4. R. Dekany, C. Neyman, and R. Flicker, “Sharpening of natural guide stars for low-order wavefront sensing using patrolling laser guide stars”, Proceedings of the SPIE, Volume 7015, pp. 701525-701525-10, 2008.
5. R. Dekany, C. Neyman, and R. Flicker, “Sharpening of natural guide stars for low-order wavefront sensing using patrolling laser guide stars”, Keck Adaptive Optics Note 601, (W. M. Keck Observatory, Kamuela, Hawaii, 2008).
6. D. Gavel, Keck Adaptive Optics Note 621, (W. M. Keck Observatory, Kamuela, Hawaii, 2008).
7. R. Dekany, “NGAO Point and Shoot Trade Study Status”, NGAO Preliminary Design phase team meeting 2, August 19, 2008, http://www.oir.caltech.edu/twiki_oir/bin/view/Keck/NGAO/080815_Remote_NGAO_PD_Meeting_2.

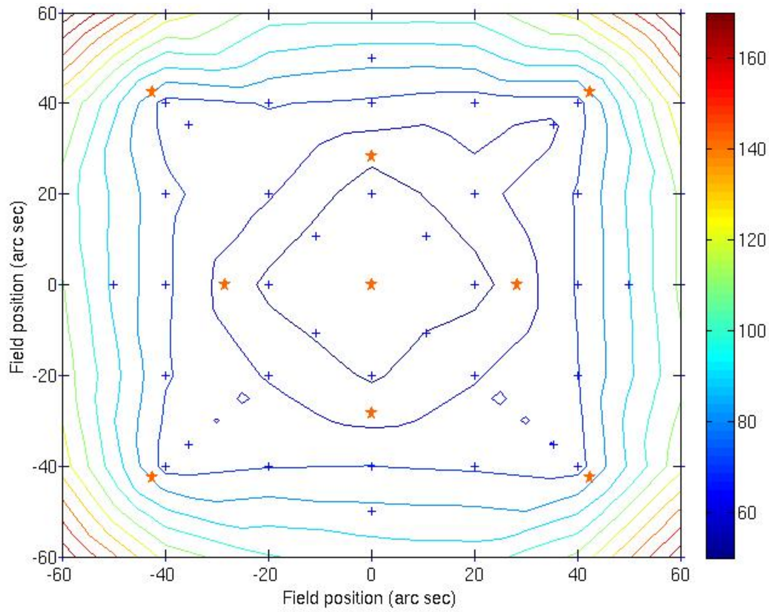

Figure 1: A nine LGS asterism, orange stars designate the location of the guide stars, the tomography error contours are spaced between 50 and 170 nm in steps of 10 nm. This asterism was designated "9c" in KAON 429 [2]. The outer square of LGS is 60 arc seconds on a side and the inner square is 40 arc seconds on a side.

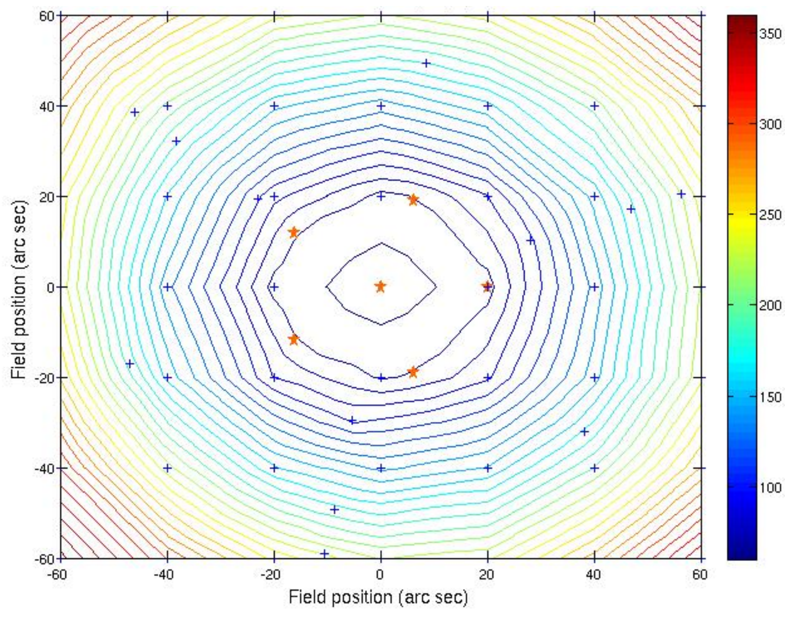

Figure 2: A 6 LGS asterism, orange stars designate the location of the guide stars, the tomography error contours are spaced between 60 and 360 nm in steps of 10 nm. This asterism was designated "Pentagon 20". The ring of LGS is at a radius of 20 arc seconds.

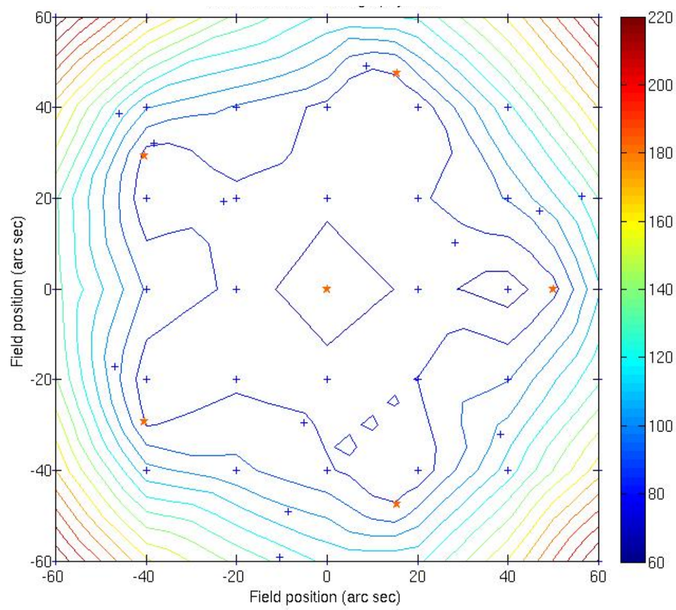

Figure 3: A 6 LGS asterism, orange stars designate the location of the guide stars, the tomography error contours are spaced between 60 and 220 nm in steps of 10 nm. This asterism was designated “Pentagon 50”. The ring of LGS is at a radius of 50 arc seconds.

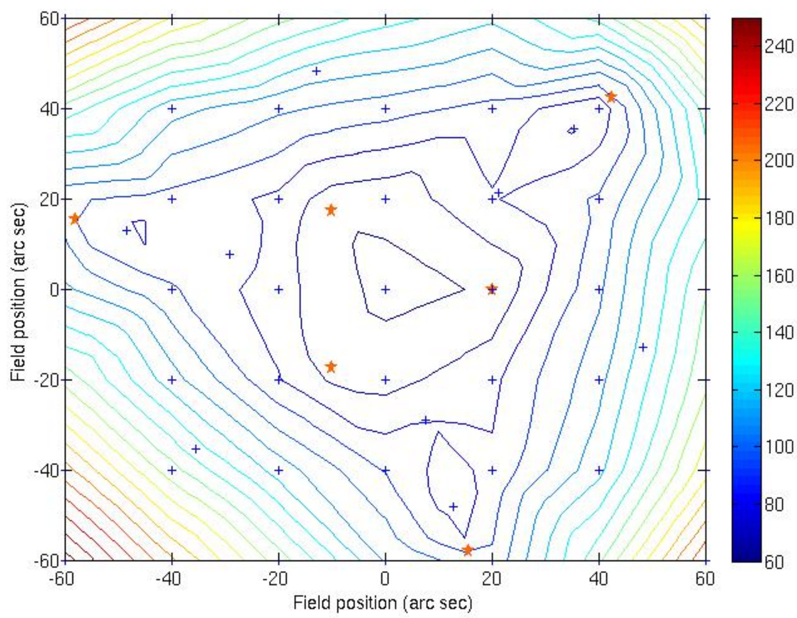

Figure 4: A 6 LGS asterism, orange stars designate the location of the guide stars, the tomography error contours are spaced between 60 and 250 nm in steps of 10 nm. This asterism was designated “3a 20 plus 3a 60”. The inner (outer) ring of LGS is at a radius of 20 (60) arc seconds. The two triangles are rotated 45 degrees to each other.

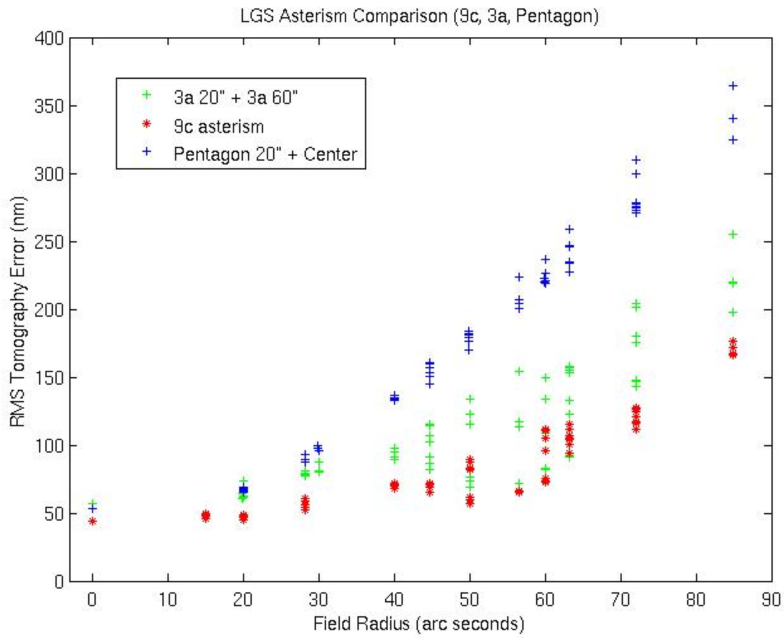

Figure 5: A comparison of the tomography errors from 9c (Figure 1), Pentagon 20 arc second (Figure 2), and 3a 20 arc second plus 3a 60 arc second (Figure 4).

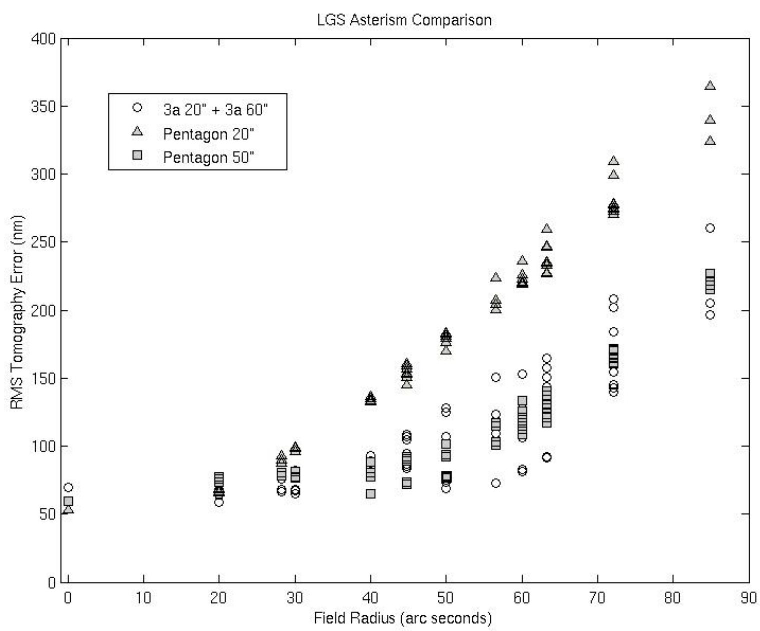

Figure 6: A comparison of the tomography errors from Pentagon 20 arc second (Figure 2), Pentagon 50 arc second (Figure 3) and 3a 20 arc second plus 3a 60 arc second (Figure 4)

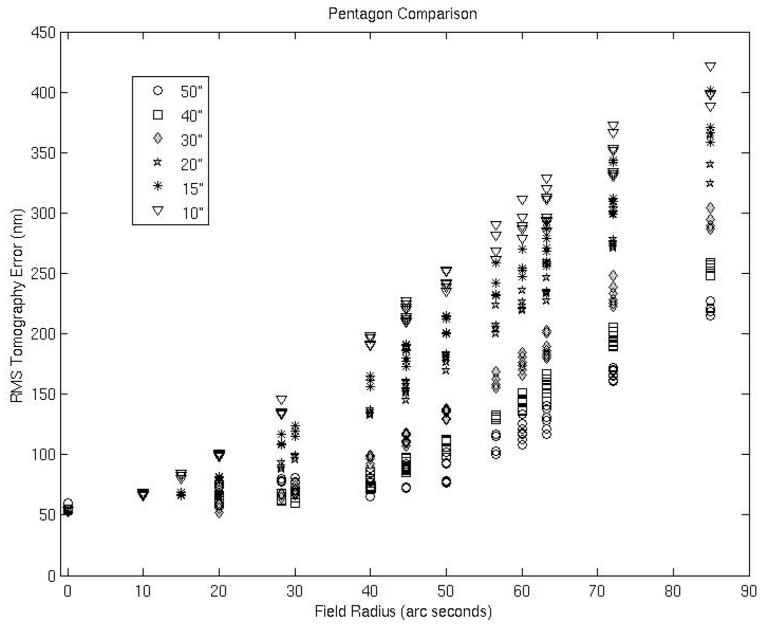

Figure 7: A comparison of the tomography errors for Pentagon (plus center) asterisms of radius from 10 to 50 arc seconds.

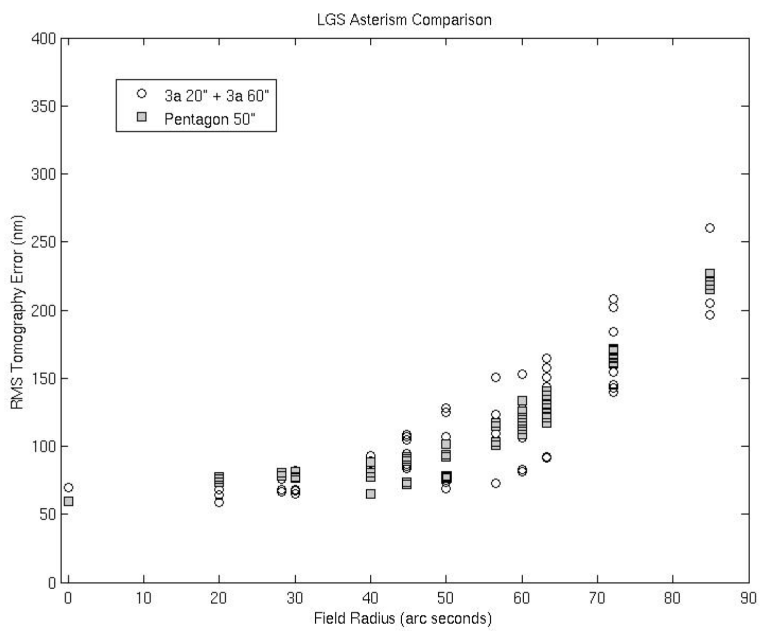

Figure 8: A comparison of the tomography errors for Pentagon (plus center) asterisms of radius from 50 arc seconds and the 3a 20 arc second plus 3a 60 arc second asterism.

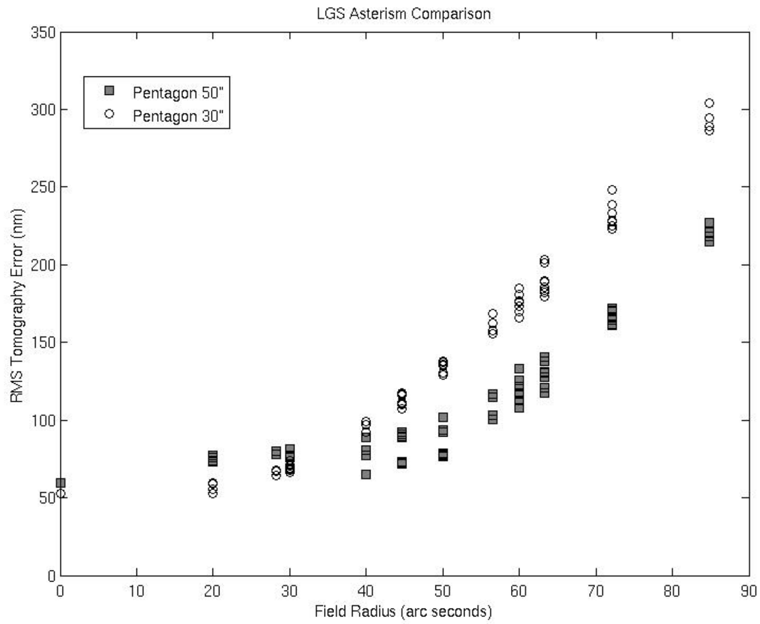

Figure 9: A comparison of the tomography errors for Pentagon (plus center) asterisms of radius from 50 arc seconds and a pentagon (plus center) of 30 arc seconds.

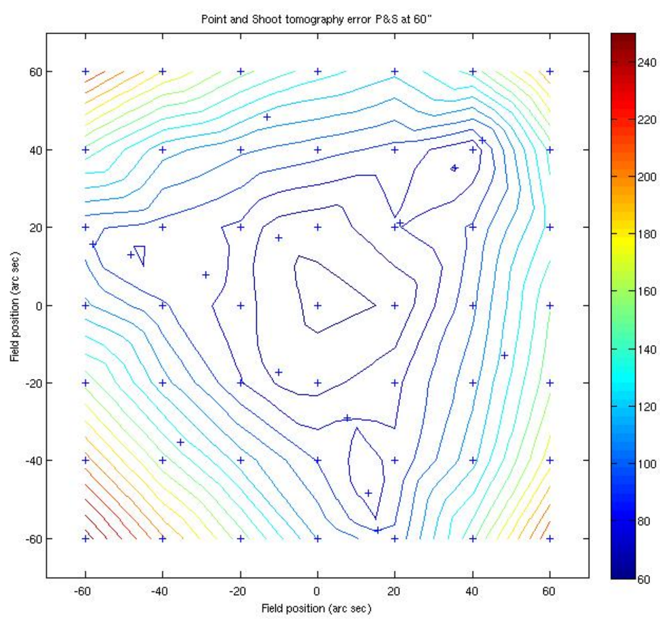

Figure 10: Tomography error contours for the 3a 20 + 3a 60 asterism. The tomography error contours are spaced between 60 and 250 nm in steps of 10 nm. This asterism was designated "3a 20 plus 3a 60". The inner (outer) ring of LGS is at a radius of 20 (60) arc seconds. The two triangles are rotated 45 degrees to each other.

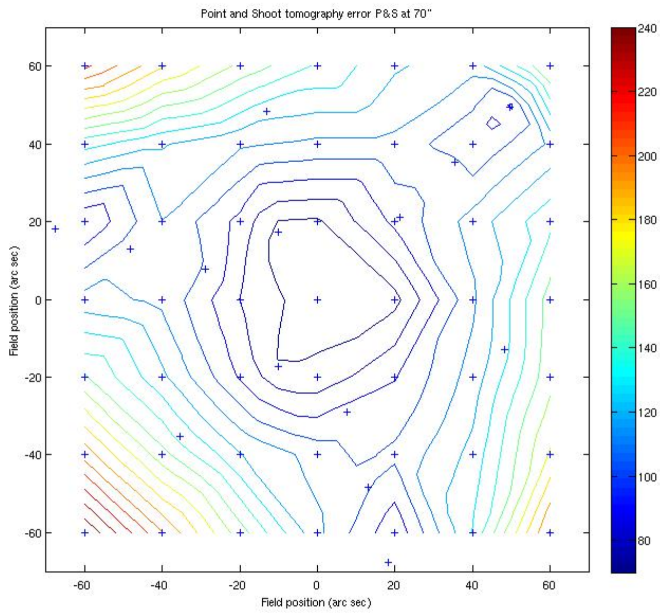

Figure 11: Tomography error contours for the 3a 20 + 3a 70 asterism. The tomography error contours are spaced between 70 and 240 nm in steps of 10 nm. This asterism was designated "3a 20 plus 3a 60". The inner (outer) ring of LGS is at a radius of 20 (60) arc seconds. The two triangles are rotated 45 degrees to each other.

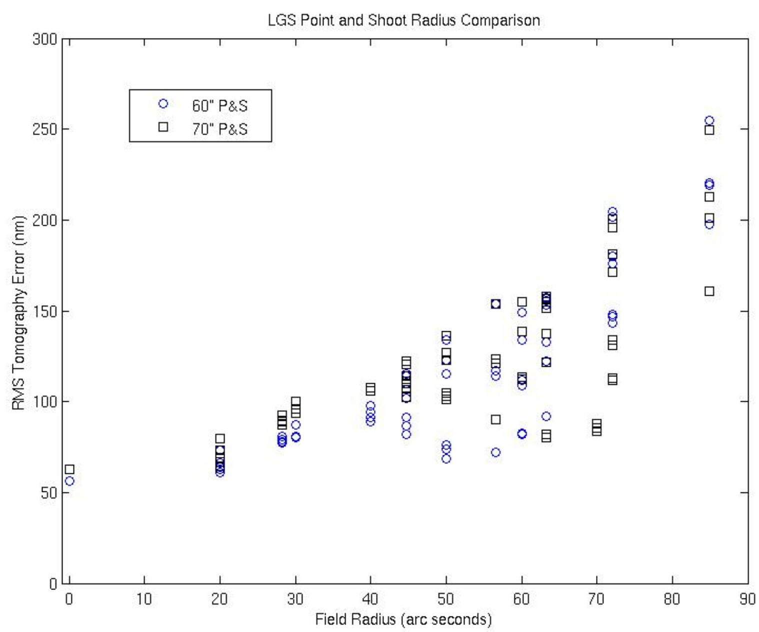

Figure 12: A comparison of the tomography errors for 3a 20 asterisms with the outer 3a asterism at 60 or 70 arc seconds radius.

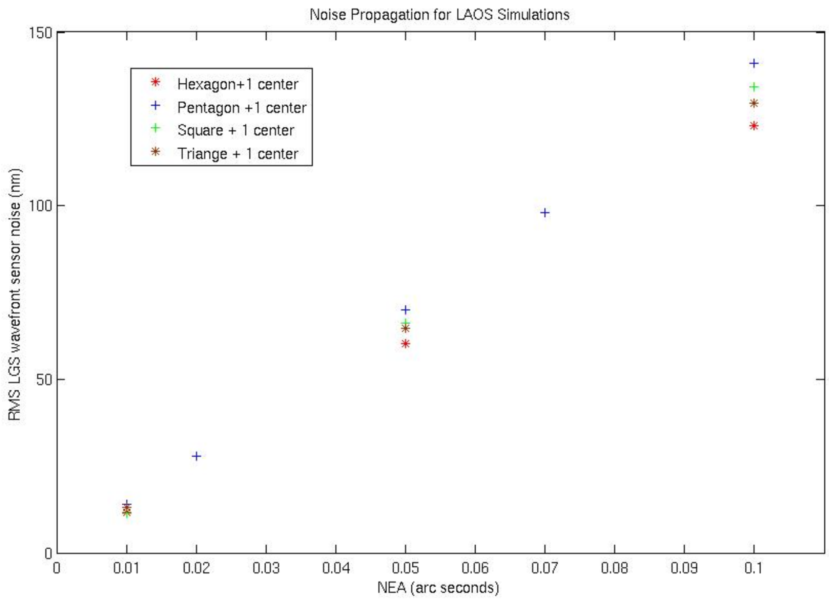

Figure 13: Noise propagation test for LGS guide stars located on a fixed ring. The LGS are located on regular polygon with one LGS at the center. The simulations show a weak dependence on LGS number.

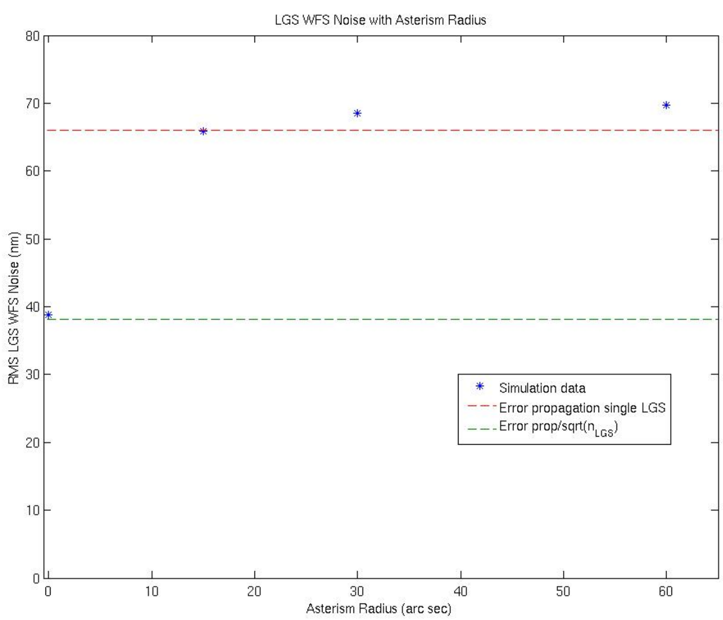

Figure 14: Noise propagation test, 3 LGS are located on a ring of increasing radius. The noise contribution increases as the beams overlap less and less as the radius is increased. At a radius of zero the system should be behave like a single guide star that is 3 time brighter. As the radius increases, a limit is reached where the wavefronts of each guide star no longer overlap and the error approaches that of a single guide star. See text and KAON 621 for more details.